Metall. Res. Technol. **111**, 221–227 (2014)
© EDP Sciences, 2014
DOI: 10.1051/metal/2014027
www.metallurgical-research.org

Metallurgical Research & Technology

Short Communication

Beneficial effect of B on hot ductility of 20CrMnTi steel with 0.05% Sn

Hongbing Peng[1], Weiqing Chen[1], Lie Chen[2] and Dong Guo[2]

[1] *State Key Laboratory of Advanced Metallurgy, University of Science and Technology Beijing, Beijing 100083, P.R. China*
e-mail: phbing1021@126.com
[2] *Xining Special Steel Co. Ltd., Xining 810005, P.R. China*

Key words:
Boron; tin; hot ductility; 20CrMnTi steel

Received 16 February 2014
Accepted 4 June 2014

Abstract – The beneficial effect of B on the hot ductility of 20CrMnTi steel with 0.05% Sn was investigated. The results show that there is a trough in the hot ductility-temperature curve. With the increase in the B content, the trough shifts to a lower temperature and becomes shallow, and the hot brittle range becomes narrow. In addition, B greatly enhancing the hot ductility was due mainly to its suppressing the Sn segregation, retarding the austenite/ferrite deformation, accelerating the onset of dynamic recrystallization (DRX) and promoting the intragranular nucleation of ferrite. Moreover, in the present case, adding 92 ppm B can nucleation of ferrite. Moreover, in the present case, adding 92 ppm B can obtain the best effect in improving the hot ductility of 20CrMnTi steel with 0.05% Sn.

With the development of the scrap-EAF (electric arc furnace) route, the adverse effect of residual elements such as tin, copper, arsenic and antimony from steel scraps has attracted extensive attention. For example, copper can cause surface hot shortness [1, 2], which is due to the copper-rich liquid penetrating into the austenite grain boundary, and when it coexists with tin, arsenic and antimony, the hot-shortness tendency will increase because they can decrease copper solubility in the austenite phase and the melting point of the copper-rich phase [3, 4]. In addition, the hot ductility loss in the temperature range of 700∼1000 °C [5–7], in which the straightening operation takes place, observed in some carbon and low alloy steels is an industrial problem [8]. In prior work [9–11], tin can deteriorate hot ductility due to its segregation to the grain boundary. Xiao et al. [12] suggested that lanthanum could improve the poor hot ductility deteriorated by tin. Boron has been considered as a possible element to enhance the hot ductility. Additionally, the content of residual element tin is high in products such as 20CrMnTi steel of Xining Special Steel Co. Ltd. Therefore, the aim of this paper is to study the effect of boron on the hot ductility of 20CrMnTi steel with 0.05% Sn; furthermore, the mechanism and the dosage of boron are discussed in detail.

1 Experimental

The chemical compositions of the steels investigated are given in Table 1. Steel ingots were prepared by laboratory vacuum induction furnace and then hot-forged into wire rods of 15 mm in diameter. Tensile test specimens with dimensions of 10 mm diameter and 120 mm gauge length were machined from the wire rods. Hot tensile tests were performed using the computerized thermal stress/strain simulator Gleeble 1500 and the reduction of area (RA) was measured to evaluate the hot ductility of the steels.

The specimens were heated from room temperature to 1350 °C at 10 °C/s, held for 300 s and then cooled to the deform temperature (*D.T.*: from 650 °C to 1050 °C with a 50 °C interval) at 3 °C/s. Specimens were held at the *D.T.* for 120 s and then

Table 1. Chemical composition of the steels examined (mass fraction, %)

steel	C	Si	Mn	P	S	Cr	Ti	Sn	B	N
B0	0.19	0.26	1.08	0.020	0.0050	1.08	0.090	0.049	0	0.0027
B1	0.21	0.26	1.08	0.017	0.0034	1.09	0.061	0.050	0.0031	0.0064
B2	0.18	0.26	1.05	0.015	0.0028	1.08	0.079	0.050	0.0058	0.0043
B3	0.19	0.26	1.06	0.015	0.0029	1.07	0.076	0.050	0.0092	0.0081

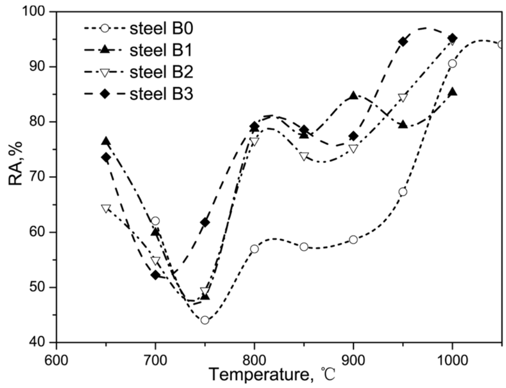

Fig. 1. Hot ductility curves for the tensile-tested steels.

strained to failure at a strain rate of 10^{-2} s^{-1}. To minimize oxidation, all tests were conducted in an inert atmosphere of Ar. After rupture, the specimens were immediately quenched by water spraying to preserve the microstructure at the *D.T*. The fractures of specimens were examined using a scanning electron microscope (SEM); the microstructures of the specimens were investigated using an optical microscope (OM) and an electron probe micro-analyzer (EPMA) was employed to study the Sn content on the substrate and at the grain boundary. It must be pointed out that the initial austenitic grain size, which is an average value of the length and width of a grain, is similar for all the four tested steels held at 1350 °C for 300 s, and the initial austenitic grain size for the four steels examined is about 240 ± 5 μm.

2 Results and discussion

2.1 Hot ductility evaluation

Figure 1 shows the curves of hot ductility against temperature for the tensile-tested steels. Apparently, there is a trough in the curve, and the hot brittle ranges for steels B0, B1, B2 and B3 are from ~702 °C to ~919 °C, from ~698 °C to ~771 °C, from ~678 °C to ~771 °C, and from ~675 °C to ~745 °C, respectively, by the rule that the temperature range in which RA is less than or equal to 60% is called the hot brittle range [6, 13]. With the increase in B content, the hot brittle range becomes narrow, and the ductility trough shifts to a lower temperature and becomes shallow. It can be inferred that the hot ductility of 20CrMnTi steel with 0.05% Sn can be enhanced significantly by the addition of B.

2.2 Microstructure and fracture morphology

Figure 2 shows the microstructures taken in the longitudinal section near the fracture. It can be seen that the proeutectoid ferrite formed along the austenite grain boundaries at 750 °C (see Figs. 2b, 2d and 2f) for steels B0, B1 and B2 and at 700 °C (see Fig. 2h) for steel B3, as the ductility trough appears at 750 °C for steels B0, B1 and B2 and it appears at 700 °C for steel B3 (see Fig. 1). Therefore, the formation of the ductility trough should be due to the proeutectoid ferrite surrounding the austenite boundaries and it is consistent with previous work [11]. Because the ferrite yield strength is relatively low compared with that of the austenite, it is easy to form a stress concentration on the ferrite film and thus greatly reduce the hot ductility. The microstructure for steels B0, B1 and B2 at 800 °C is martensite (see Figs. 2a, 2c and 2e), while that for steel B3 is at 750 °C (see Fig. 2g). This means that 92 ppm B in steel B3 can suppress the formation of proeutectoid ferrite, and retard austenite/ferrite transformation because the chemical compositions of the steels examined are nearly identical except for B content. Moreover, compared with the microstructure of steel B0 tensile-tested at 700 °C (see Fig. 2i), a large quantity of intra-granular ferrite (IGF) was found in the austenite grain interior in steel B3 tensile-tested at 700 °C (see Fig. 2h), which means that adding B can promote the intragranular nucleation of ferrite.

Figure 3 shows the fracture morphology tensile-tested at 750 °C for steel B0

https://doi.org/10.1051/metal/2014027 Published online by Cambridge University Press

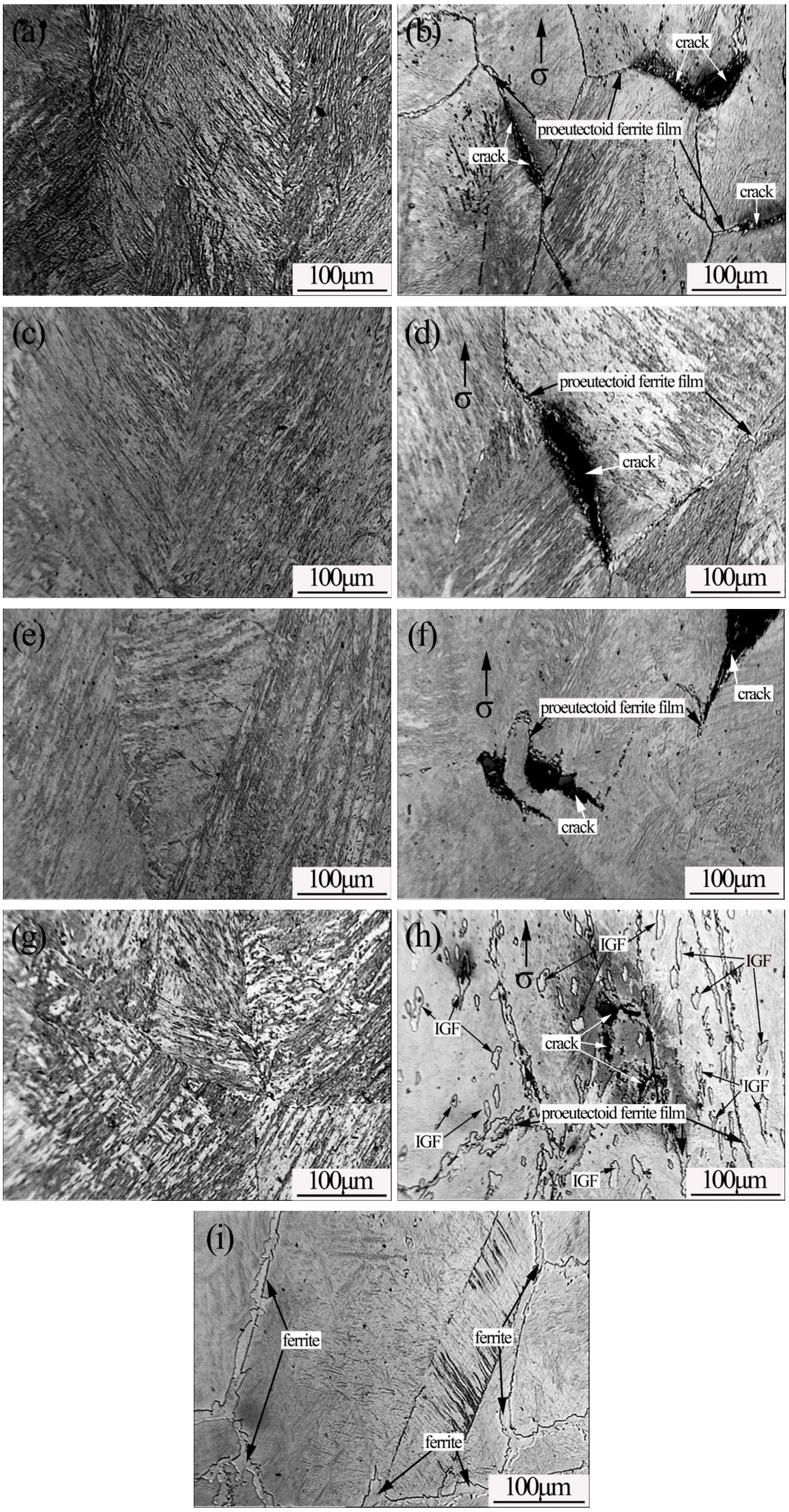

Fig. 2. Optical microstructures for steel B0 ((a) tensile-tested at 800 °C, (b) tensile-tested at 750 °C and (i) tensile-tested at 700 °C), steel B1 ((c) tensile-tested at 800 °C and (d) tensile-tested at 750 °C), steel B2 ((e) tensile-tested at 800 °C and (f) tensile-tested at 750 °C) and steel B3 ((g) tensile-tested at 750 °C and (h) tensile-tested at 700 °C).

https://doi.org/10.1051/metal/2014027 Published online by Cambridge University Press

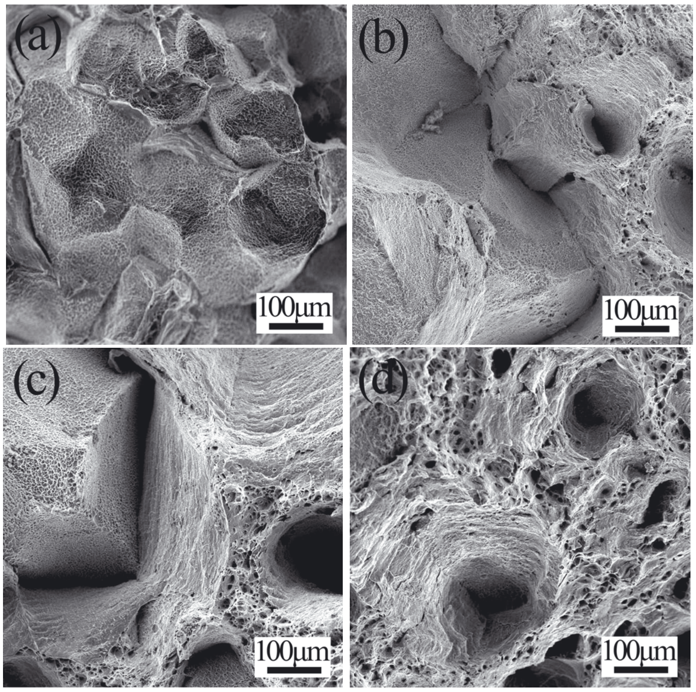

Fig. 3. Fracture morphology at 750 °C for (a) steel B0, (b) steel B1, (c) steel B2 and (d) steel B3.

Table 2. Results of quantitative analysis of steel B3 tested by EPMA (mass fraction %).

points	1	2	3	4	5	6	avg.	*SD*	*SEA*
Boundary Sn	0.084	0.017	0.089	0.02	0.071	0.024	0.051	0.034	0.014
Substrate Sn	0.117	0.084	0.089	0.054	0.074	0.021	0.073	0.033	0.013

Note: Standard deviation, $SD = \sqrt{Var}$, where $Var = \frac{1}{n-1}\sum_{i=1}^{n}\left(C_i - C_{avg.}\right)^2$, Standard error of the average, $SEA = \frac{SD}{\sqrt{n}}$; and $n = 6$.

(see Fig. 3a), steel B1 (see Fig. 3b), steel B2 (see Fig. 3c) and steel B3 (see Fig. 3d). The fracture for steel B0 exhibits completely intergranular failure and the facets are quite smooth, indicating that the ductility is severely deteriorated by Sn [11]. Moreover, the fracture morphology is changed to ductile failure gradually with the increase in B content and the fracture appears to be a ductile fracture with many dimples and without grain boundary facets for steel B3. The fracture morphology is well coincident with the hot ductility, i.e., the worse the hot ductility, the greater the severity of the intergranular failure.

2.3 EPMA analysis

The value of RA was increased from ~67% in steel B0 to ~95% in steel B3 due to the addition of B, particularly at 950 °C. Therefore, two metallographic specimens were taken in the longitudinal section near the fracture from steel B3 tensile-tested at 950 °C. One was eroded with picric acid for a random spot scan at the grain boundaries examined by electron probe micro-analyzer (EPMA) and the other was not eroded with picric acid for the random spot scan on the substrate. The results can be seen in Table 2 and Figure 4; the value of $(B/S)_{Sn}$ is 0.70, and this means there is no significant Sn segregation at the grain boundaries in steel B3. The average content of Sn at the grain boundary/that on the substrate was defined as $(B/S)_{Sn}$. However, according to the same method, there is significant Sn segregation at the grain boundaries in steel B0 tensile-tested at 950 °C and the value of $(B/S)_{Sn}$ is 2.4. Therefore, it can be inferred

https://doi.org/10.1051/metal/2014027 Published online by Cambridge University Press

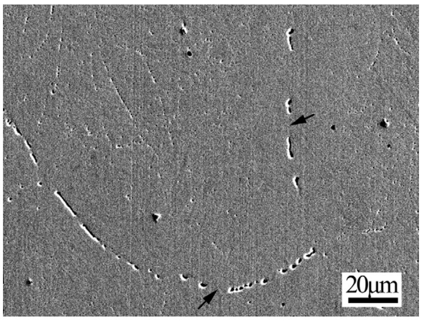

Fig. 4. Spot scan by EPMA at the grain boundary of steel B3.

that Sn segregation at the grain boundaries is suppressed by the addition of B.

3 Discussion

0.049%Sn in steel B0 greatly deteriorating the hot ductility of 20CrMnTi steel is due mainly to Sn segregation at the grain boundary, which reduces the surface energy of the grain boundary, weakens intergranular cohesion, accelerates nucleation and growth of the grain boundary voids, and impedes the grain boundary migration and DRX, and it has been described in detail in previous work [11].

In the present case, as the chemical compositions of the steels examined are nearly identical except the B content, therefore, the difference in the value of $(B/S)_{Sn}$ between steel B0 and steel B3 should be due to the B addition and the improvement in hot ductility should arise from B non-equipment segregation at grain boundaries [14]. B-vacancy complexes formed due to the excess vacancies produced by deformation. The complexes migrate to grain boundaries and are annihilated preferentially at the boundaries as the B-vacancy binding energy, $E_B \approx 0.5$ eV [15], is considerably higher than the B-dislocation binding energy, but lower than the B-grain boundary segregation energy, E_{gb}, which is estimated to be 0.65 eV [16]. Thus, in spite of the high dislocation density during deformation, the dissociation of B-vacancy complexes does not take place or is of negligible importance in grain interiors. Also, the diffusivity of the complexes is about one order of magnitude higher than that of solute B so that negligible desegregation occurs during the enrichment period [15]. Therefore, there should be a considerable B segregation at austenite grain boundaries during deformation. Moreover, according to the fact that the value of $(B/S)_{Sn}$ is decreased from 2.4 to 0.70 due to B addition, it is inferred that B segregation to the austenite boundary can be very effective in displacing Sn, as B suppressing Sn segregation at austenite grain boundaries is due to its large free energy of segregation, presumably about 100 kJ/mol, which affects segregation of Sn, with a free energy of about 50 kJ/mol [17]. Therefore, the adverse effect of Sn segregation to grain boundaries on the hot ductility is reduced or even eliminated. In addition, prior work [18–20] has reported that B segregating to austenite grain boundaries changes the thermodynamic characteristics of these boundaries and this may have some effect on the softening behavior of austenite during hot working, and hence have a beneficial effect on hot ductility. Laha et al. [19] assumed that boron is concentrated at the grain boundaries where microcavity formation was suppressed; moreover, B addition to the steel decreased the cavity growth rate by almost an order of magnitude and B atoms segregating at the boundary can act as a type of "glue" [20], which can enhance the grain boundary cohesion and prevent the steel from failing. Furthermore, B can accelerate the onset of DRX, as shown in Figure 5. The reason for this could be related to the character of the B atom, as an interstitial atom which may promote a diminution of the activation energy, therefore accelerating the onset of DRX [21].

B enhancing the hot ductility of 20CrMnTi steel with 0.05% Sn can also be ascribed to retardation of the austenite/ferrite transformation, which presumably avoids ferrite film formation at the austenite grain boundaries, increasing the resistance to grain boundary sliding during the straightening operation, which results in better creep ductility [22]. In addition, a large quantity of intra-granular ferrite (IGF) was found in the austenite grain interior in steel B3 compared with that of steel B0, as illustrated in Figures 2h and 2i. According to Kim et al. [23], $Fe_{23}(B,C)_6$ particles can appear in the austenite grains in B-containing steel and

https://doi.org/10.1051/metal/2014027 Published online by Cambridge University Press

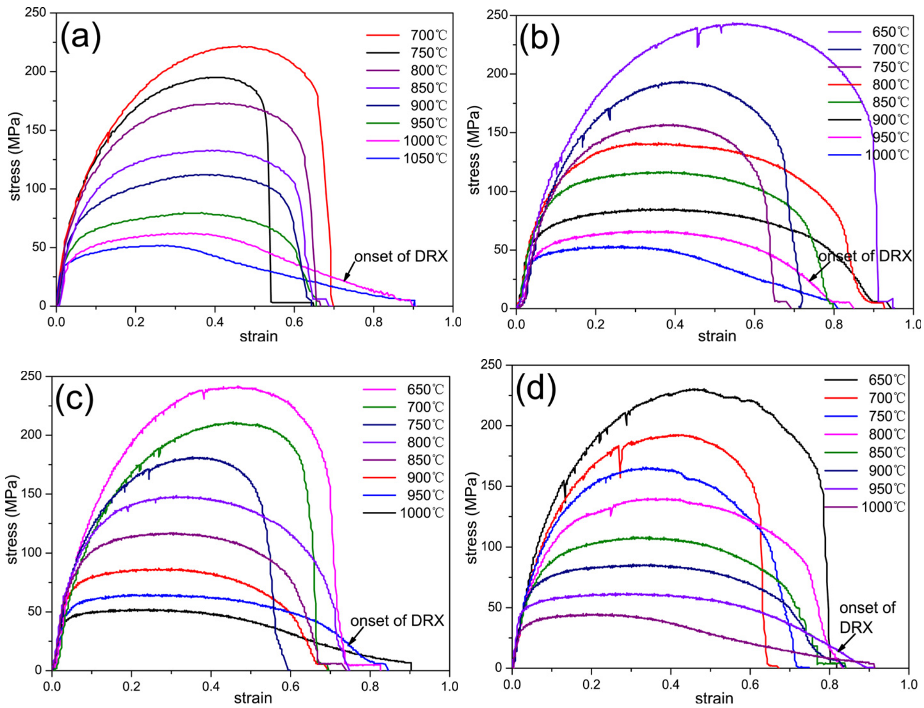

Fig. 5. Flow curves of stress-strain during tensile tests for (a) steel B0, (b) steel B1, (c) steel B2 and (d) steel B3.

these matrix particles act as the preferential sites for the intragranular nucleation of ferrite. In the present case, some of the particles are associated with IGF (see Fig. 2h), so it can be inferred that adding B to steel could cause the formation of particles containing B which can act as a preferential site for IGF. Thus, adding B to 20CrMnTi steel with 0.05% Sn can promote the intragranular nucleation of ferrite and make the austenite grain interior more deformable, and alleviates strain concentration at the grain boundaries because of the soft IGF, and hence it can improve the hot ductility significantly. Furthermore, in the present case, it can be seen that adding 92 ppm B to 20CrMnTi steel with 0.05% Sn can obtain the best effect in improving the hot ductility.

4 Conclusions

The beneficial effect of B on hot ductility of 20CrMnTi steel with 0.05% Sn was investigated by means of a Gleeble 1500 thermomechanical simulator. The results show that there is a trough in the hot ductility curve. With the increase in the B content, the trough shifts to a lower temperature and becomes shallow, and the hot brittle range becomes narrow. In addition, B greatly enhancing the hot ductility was due mainly to its suppressing the Sn segregation, retarding the austenite/ferrite deformation, accelerating the onset of dynamic recrystallization (DRX) and promoting the intragranular nucleation of ferrite. Moreover, in the present case, adding 92 ppm B can obtain the best effect in improving the hot ductility of 20CrMnTi steel with 0.05% Sn.

References

[1] L.G. Garza, C.J. Van Tyne, *J. Mater. Process. Tech.* **159** (2005) 169
[2] L. Yin, S. Sridhar, *Metall. Mater. Trans. B* **42** (2011) 1031
[3] H. Okamoto, Desk Handbook: Phase Diagrams for Binary Alloys, ASM International, Materials Park, OH, 2000
[4] J.M.J. Salter, *J. Iron Steel Inst.* **204** (1966) 478
[5] B. Mintz, *ISIJ Int.* **39** (1999) 833
[6] B. Mintz, S. Yue, J.J. Jonas, *Int. Mater. Rev.* **36** (1991) 187
[7] B. Mintz, D.N. Crowther, *Int. Mater. Rev.* **55** (2010) 168

https://doi.org/10.1051/metal/2014027 Published online by Cambridge University Press

[8] B. Mintz, J.R. Wilcox, D.N. Crowther, *Mater. Sci. Technol.* **2** (1986) 589
[9] Z.X. Yuan, J. Jia, A.M. Guo et al., *Acta Metall. Sin.* 1**6** (2004) 478
[10] S. Song, Z. Yuan, J. Jia et al., *Metall. Mater. Trans. A* **34** (2003) 1611
[11] H. Peng, W. Chen, L. Chen et al., *High Temp. Mater. Processes* **33** (2014) 179
[12] X. Jiguang, W. Fuming, L. Changrong et al., *J. Chin. Rare. Earth.* **25** (2007) 278
[13] S. Song, A. Guo, D. Shen et al., *Mat. Sci. Eng. A* **360** (2003) 96
[14] F. Zarandi, S. Yue, *ISIJ Int.* **46** (2006) 591
[15] L. Karlsson, *Acta Metall.* **36** (1988) 25
[16] L. Karlsson, H. Nordén, *Acta Metall.* **36** (1988) 13
[17] S. Suzuki, K. Kuroki, H. Kobayashi et al., *Mater. Trans. JIM* **33** (1992) 1068
[18] E.D. Hondros, M.P. Seah, *Int. Met. Rev.* **22** (1977) 262
[19] K. Laha, J. Kyono, S. Kishimoto et al., *Scripta Mater.* **52** (2005) 675
[20] M.K. Miller, P.J. Pareige, K.F. Russell, an Oak Ridge National Laboratory Report, 2001, TN.
[21] I.A.I. Mej, A. Bedolla-Jacuinde, C.E.M. Maldonado et al., *Mat. Sci. Eng. A* **528** (2011) 4468
[22] N.E. Hannerz, *Trans. Iron Steel Inst. Jpn* **25** (1985) 149
[23] S.K. Kim, N.J. Kim, J.S. Kim, *Metall. Mater. Trans. A* **33** (2002) 701

https://doi.org/10.1051/metal/2014027 Published online by Cambridge University Press